Vol 14 No 11, November 2005
1009-1963/2005/14(11)/2305-09

Chinese Physics

© 2005 Chin. Phys. Soc.
and IOP Publishing Ltd

# Scattering characteristics of conducting cylinder coated with nonuniform magnetized ferrite*

Hu Bin-Jie(胡斌杰)[a], Edward Yung Kai-Ning(容启宁)[b], Zhang Jun(张 军)[c]†, and Toutain Serge[d]

[a] *South China University of Technology, Guangzhou 510640, China*
[b] *City University of Hong Kong, Kowloon, Hong Kong SAR, China*
[c] *Sun Yat-Sen University, Guangzhou 510275, China*
[d] *University of Nantes, Nantes 44306, France*

(Received 4 December 2004; revised manuscript received 27 June 2005)

An analytical technique, referred to as the scattering matrix method (SMM), is developed to analyse the scattering of a planar wave from a conducting cylinder coated with nonuniform magnetized ferrite. The SMM solution for the nonuniform ferrite coating can be reduced to the expressions for the scattering and penetrated coefficients in four particular cases: nonuniform magnetized ferrite cylinder, uniform magnetized ferrite-coated conducting cylinder, uniform ferrite cylinder as well as homogeneous dielectric-coated conducting cylinder. The resonant condition for the nonuniform ferrite coating is obtained. The distinctive differences in scattering between the nonuniform ferrite coating and the nonuniform dielectric coating are demonstrated. The effects of applied magnetic fields and wave frequencies on the scattering characteristics for two types of the linear profiles are revealed.

**Keywords:** scattering, inhomogeneous ferrite, conducting cylinder; scattering matrix method
**PACC:** 7220D, 1220, 0200

## 1. Introduction

Electromagnetic wave scatterings from inhomogeneous gyroelectric and gyromagnetic objects have recently received much attention because of their importance in many practical areas.[1−6] Various problems of scattering by ferrite cylindrical objects have been investigated in the past years. These include the scatterings by a homogeneous magnetized ferrite cylinder[7−9] and a finite periodic structure of homogeneous ferrite cylinders,[10] the scattering by a conducting circular cylinder coated with homogeneous ferrite,[11,12] and the scattering by the ferrite post in a waveguide.[13−15] However, few researchers have reported the scattering by nonuniform ferrite-coated conducting cylinders.

In this paper the scattering of a planar wave from a conducting cylinder coated with nonuniform magnetized ferrite is investigated by a so-called scattering matrix method originally employed by Helaly and later by the authors to deal with plasma problems.[1,4] In this method, the nonuniform ferrite-coated conducting cylinder is first divided into many layers. Then each layer can be considered as a uniform one and its scattering matrix is derived based on the field continuity condition. Finally the scattering matrix of the whole nonuniform ferrite-coated conducting cylinder can be synthesized using the scattering matrix for each layer. Since the endocentric recursion technique is adopted in the approach, the so-derived formulae for the nonuniform ferrite-coated conducting cylinders can easily degenerate into the formulae for the nonuniform ferrite cylinders. The characteristics of scattering by ferrite-coated conducting cylinders with linear profiles are investigated versus applied magnetic fields and wave frequencies. The distinctive differences between the ferrite coating and the dielectric coating are demonstrated.

## 2. Formulation

Consider the scattering of a TM wave normally

*Project supported by Specialized Research Fund for the Doctoral Program of Higher Education, China (Grant No 20020561024), and Guangzhou Science and Technology Project of China (Grant No 2005J1-C0061).

†Corresponding author. E-mail: junzhang@ieee.org

incident upon a nonuniform ferrite-coated conducting cylinder as shown in Fig.1, where the nonuniform-coated ferrite is divided into $p$ layers.

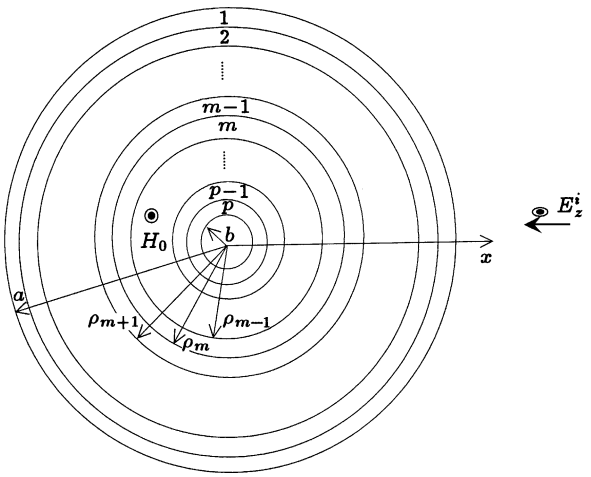



**Fig.1.** Geometry of the problem.

A magnetic bias field $H_0$ is applied in the $z$ direction, thus the permeability tensor in the $m$th layer is[16,17]

$$\left[\mu^{(m)}\right] = \begin{bmatrix} \mu_1^{(m)} & \mathrm{j}\mu_2^{(m)} & 0 \\ -\mathrm{j}\mu_2^{(m)} & \mu_1^{(m)} & 0 \\ 0 & 0 & \mu_0 \end{bmatrix} \tag{1}$$

with

$$\mu_1^{(m)} = \mu_0\left(1 + \frac{\omega_{\mathrm{M}}^{(m)}(\omega_0^{(m)} + \mathrm{j}\omega\alpha^{(m)})}{(\omega_0^{(m)} + \mathrm{j}\omega\alpha^{(m)})^2 - \omega^2}\right), \tag{2}$$

$$\mu_2^{(m)} = \mu_0\frac{\omega\omega_{\mathrm{M}}^{(m)}}{(\omega_0^{(m)} + \mathrm{j}\omega\alpha^{(m)})^2 - \omega^2}, \tag{3}$$

where $\omega_0^{(m)} = \gamma\mu_0 H_0^{(m)}$ is the precession frequency, $\omega_m = \gamma\mu_0 M_0^{(m)}$, and $\omega$, $\gamma$, $M_0^{(m)}$, $\alpha^{(m)}$, and $\mu_0$ are the wave frequency, the gyromagnetic ratio, the saturation magnetization, the damping factor and the permeability in free space, respectively. It is known that the electric field of the incident TM wave can be written in the following form:

$$E_z^{\mathrm{i}} = E_0\mathrm{e}^{-\mathrm{j}k_0\rho\cos\varphi}, \tag{4}$$

which can be expanded in terms of the Bessel function $J_n$ as

$$E_z^{\mathrm{i}} = E_0\sum_{n=-\infty}^{+\infty}(-\mathrm{j})^n J_n(k_0\rho)\mathrm{e}^{-\mathrm{j}n\varphi}, \tag{5}$$

where $E_0$ is the amplitude and $k_0$ is the wave number in free space. The scattered electric field in free space can be written as

$$E_z^{\mathrm{s}} = E_0\sum_{n=-\infty}^{+\infty}A_n(-\mathrm{j})^n H_n^{(2)}(k_0\rho)\mathrm{e}^{-\mathrm{j}n\varphi}, \tag{6}$$

where $A_n$ are coefficients to be determined and $H_n^{(2)}$ are the Hankel functions of the second kind. Thus the total field in the incident region is obtained:

$$\begin{aligned} E_z =& E_z^{\mathrm{i}} + E_z^{\mathrm{s}} \\ =& E_0\sum_{n=-\infty}^{+\infty}(-\mathrm{j})^n[J_n(k_0\rho) + A_n H_n^{(2)}(k_0\rho)]\mathrm{e}^{-\mathrm{j}n\varphi}. \end{aligned} \tag{7}$$

In the $m$th ferrite layer, the total electric field can be written as[17]

$$\begin{aligned} E_z^{(m)} =& E_0\sum_{n=-\infty}^{+\infty}(-\mathrm{j})^n[B_n^{(m)}J_n(k_{\mathrm{e}}^{(m)}\rho) \\ &+ C_n^{(m)}H_n^{(2)}(k_{\mathrm{e}}^{(m)}\rho)]\mathrm{e}^{-\mathrm{j}n\varphi}, \end{aligned} \tag{8}$$

where

$$k_{\mathrm{e}}^{(m)} = \omega\sqrt{\varepsilon^{(m)}(\mu_1^{(m)2} - \mu_2^{(m)2})/\mu_1^{(m)}} = \omega\sqrt{\varepsilon^{(m)}\mu_{\mathrm{e}}^{(m)}}$$

is an effective wave number in the $m$th layer, and $B_n^{(m)}$and $C_n^{(m)}$ are unknown coefficients. For convenience, we define $Y_{\mathrm{e}}^{(m)} = \sqrt{\varepsilon^{(m)}/\mu_{\mathrm{e}}^{(m)}}$ as an effective admittance in the $m$th layer. Applying the field continuity condition at $\rho = \rho_1$ leads to the following matrix equation:

$$\begin{Bmatrix} B_n^{(1)} \\ C_n^{(1)} \end{Bmatrix} = [S_1]\begin{Bmatrix} A_n \\ 1 \end{Bmatrix} \tag{9}$$

with

$$[S_1] = \begin{bmatrix} J_n(k_{\mathrm{e}}^{(1)}\rho_1) & H_n^{(2)}(k_{\mathrm{e}}^{(1)}\rho_1) \\ Y_{\mathrm{e}}^{(1)}J^{(1)}(n, k_{\mathrm{e}}^{(1)}\rho_1) & Y_{\mathrm{e}}^{(1)}H^{(1)}(n, k_{\mathrm{e}}^{(1)}\rho_1) \end{bmatrix}^{-1} \times \begin{bmatrix} H_n^{(2)}(k_0\rho_1) & J_n(k_0\rho_1) \\ Y_0 H'^{(2)}_n(k_0\rho_1) & Y_0 J'_n(k_0\rho_1) \end{bmatrix}, \tag{10}$$

where $Y_0 = \sqrt{\varepsilon_0/\mu_0}$ is a characteristic admittance in free space, the superscript " $'$ " denotes the derivative operator, and the functions of $J^{(1)}(n,x)$ and $H^{(1)}(n,x)$ are defined as

$$J^{(1)}(n,x) = J'_n(x) - \frac{\mu_2^{(1)}}{\mu_1^{(1)}}\frac{n}{x}J_n(x), \tag{11a}$$

$$H^{(1)}(n,x) = H'_n(x) - \frac{\mu_2^{(1)}}{\mu_1^{(1)}}\frac{n}{x}H_n(x). \tag{11b}$$

Similarly, by applying the field continuity condition at the $m$th interface, the following matrix equation is obtained:

$$\begin{Bmatrix} B_n^{(m)} \\ C_n^{(m)} \end{Bmatrix} = [S_m] \begin{Bmatrix} B_n^{(m-1)} \\ C_n^{(m-1)} \end{Bmatrix} \tag{12}$$

with

$$[S_m] = \begin{bmatrix} J_n(k_e^{(m)}\rho_m) & H_n^{(2)}(k_e^{(m)}\rho_m) \\ Y_e^{(m)}J^{(m)}(n,k_e^{(m)}\rho_m) & Y_e^{(m)}H^{(m)}(n,k_e^{(m)}\rho_m) \end{bmatrix}^{-1} \times \begin{bmatrix} J_n(k_e^{(m-1)}\rho_m) & H_n^{(2)}(k_e^{(m-1)}\rho_m) \\ Y_e^{(m-1)}J^{(m-1)}(n,k_e^{(m-1)}\rho_m) & Y_e^{(m-1)}H^{(m-1)}(n,k_e^{(m-1)}\rho_m) \end{bmatrix}, \tag{13}$$

where the functions of $J^{(m)}(n,x)$and $H^{(m)}(n,x)$ are similar to those in the expressions (11a) and (12b) by replacing subscript "(1)" by "$(m)$". To satisfy the boundary condition of a vanishing tangential electric field at $\rho = b$, the electric field for the $p$th layer is expressed as

$$E_z^p = E_0 \sum_{n-\infty}^{+\infty} (-\mathrm{j})^n D_n \left[ J_n(k_e^{(p)}\rho) - \frac{J_n(k_e^{(p)}b)}{H_n^{(2)}(k_e^{(p)}b)} H_n^{(2)}(k_e^{(p)}\rho) \right] \mathrm{e}^{-\mathrm{i}n\varphi}, \tag{14}$$

where $D_n$ are the unknown coefficients. Applying the field continuity condition at the $p$th interface yields

$$\begin{Bmatrix} B_n^{(p-1)} \\ C_n^{(p-1)} \end{Bmatrix} = \{V_p\}\{D_n\} \tag{15}$$

with

$$\{V_p\} = \begin{bmatrix} J_n(k_e^{(p-1)}\rho_p) & H_n^{(2)}(k_e^{(p-1)}\rho_p) \\ Y_e^{(p-1)}J^{(p-1)}(n,k_e^{(p-1)}\rho_p) & Y_e^{(p-1)}H^{(p-1)}(n,k_e^{(p-1)}\rho_p) \end{bmatrix}^{-1} \times \begin{bmatrix} J_n(k_e^{(p)}\rho_p) - \dfrac{J_n(k_e^p b)}{H_n^{(2)}(k_e^p b)} H_n^{(2)}(k_e^{(p)}\rho_p) \\ Y_e^{(p)}\left[J^{(p)}(n,k_e^{(p)}\rho_p) - \dfrac{J_n(k_e^p b)}{H_n^{(2)}(k_e^p b)} H^{(p)}(n,k_e^{(p)}\rho_p)\right] \end{bmatrix}. \tag{16}$$

Using Eqs.(9) and (12) recursively, Eq.(15) becomes

$$[S_g] \begin{Bmatrix} A_n \\ 1 \end{Bmatrix} = \{V_p\}\{D_n\}, \tag{17}$$

where $[S_g]$ is the global scattering matrix given by

$$[S_g] = \left( \prod_{m=p-1}^{2} [S_m] \right) [S_1]. \tag{18}$$

To obtain the explicit formulae of the scattering and penetrating coefficients $A_n$, $D_n$, we rewrite Eq.(18) as

$$\begin{bmatrix} \{S_{g1}\} & \{S_{g2}\} \end{bmatrix} \begin{Bmatrix} A_n \\ 1 \end{Bmatrix} = \{V_p\}\{D_n\}. \tag{19}$$

Hence the scattering and penetrating coefficients $A_n$, and $D_n$ can be solved

$$\begin{Bmatrix} A_n \\ D_n \end{Bmatrix} = -\begin{bmatrix} \{S_{g1}\} & \{-V_p\} \end{bmatrix}^{-1} \{S_{g2}\}. \tag{20}$$

Formulae (10), (13), (16), (18) and (20) are the SMM expressions for the scattering and penetrated coefficients of the nonuniform ferrite-coated conducting cylinder. To obtain SMM formulae for the nonuniform ferrite cylinder, we only let the inner radius $b$ of the conducting cylinder approach to zero, then the expression (16) reduces to[4]

$$\{V_p\} = \begin{bmatrix} J_n(k_{\rm e}^{(p-1)}\rho_p) & H_n^{(2)}(k_{\rm e}^{(p-1)}\rho_p) \\ Y_{\rm e}^{(p-1)}J^{(p-1)}(n,k_{\rm e}^{(p-1)}\rho_p) & Y_{\rm e}^{(p-1)}H^{(p-1)}(n,k_{\rm e}^{(p-1)}\rho_p) \end{bmatrix}^{-1} \times \begin{bmatrix} J_n(k_{\rm e}^{(p)}\rho_p) \\ Y_{\rm e}^{(p)}J^{(p)}(n,k_{\rm e}^{(p)}\rho_p) \end{bmatrix}. \tag{21}$$

From the above discussion we can see that the SMM formulae for the nonuniform ferrite-coated conducting cylinder and for the nonuniform ferrite cylinder have the same expressions except for the vector $V_p$, which is due to the fact that the endocentric recursion technique is adopted in the approach.

After the scattering coefficients are determined, we can easily calculate our quantity concerned, the scattering cross-section (SCS). Using the large argument approximation of the Hankel function in the expression (6), the normalized scattering cross-section (NSCS) can be obtained as follows:[18]

$$\frac{\sigma}{\lambda_0} = \frac{2}{\pi}\left|\sum_{n=-\infty}^{\infty} A_n {\rm e}^{-{\rm j}n\varphi}\right|^2, \tag{22}$$

where $\lambda_0$ is the wavelength in free space.

To confirm the correctness of the above-derived formulae for the ferrite coating, let us consider the degenerated form of the above formulae for a uniform case. If the coated-ferrite is uniform, namely $\mu_1^{(m)} = \mu_1^{(m-1)} = \ldots = \mu_1^{(1)}$, $\mu_2^{(m)} = \mu_2^{(m-1)} = \ldots = \mu_2^{(1)}$, thus $k_{\rm e}^{(m)} = k_{\rm e}^{(m-1)} = \ldots = k_{\rm e}^{(1)}$ and $Y_{\rm e}^{(m)} = Y_{\rm e}^{(m-1)} = \ldots = Y_{\rm e}^{(1)}$. Substituting these relations into the expressions (13), (16) and (18), we have

$$[S_m] = \begin{bmatrix} 1 & 0 \\ 0 & 1 \end{bmatrix},$$

$$\{V_p\} = \begin{Bmatrix} 1 \\ -J_n(k_{\rm e}^{(1)}b)/H_n^{(2)}(k_{\rm e}^{(1)}b) \end{Bmatrix}, \quad [S_g] = [S_1]\ . \tag{23}$$

After some mathematic manipulations, the expression (20) can be simplified as follows:

$$\begin{aligned} A_n =& \frac{1}{\Delta}\{J^{(1)}(n,k_{\rm e}^{(1)}\rho_1)J_n(k_0\rho_1)Y_1 \\ &- J_n'(k_0\rho_1)J_n(k_{\rm e}^{(1)}\rho_1)Y_0 \\ &+ \frac{J_n(k_{\rm e}^{(1)}b)}{H_n^{(2)}(k_{\rm e}^{(1)}b)}[J_n'(k_0\rho_1)H_n^{(2)}(k_{\rm e}^{(1)}\rho_1)Y_0 \\ &- H^{(1)}(n,k_{\rm e}^{(1)}\rho_1)J_n(k_0\rho_1)Y_1]\} \end{aligned} \tag{24a}$$

and

$$D_n = \frac{-1}{\Delta}\left(\frac{2{\rm j}Y_0}{\pi\, k_0\rho_1}\right) \tag{24b}$$

with

$$\begin{aligned} \Delta =& H_n'^{(2)}(k_0\rho_1)J_n(k_{\rm e}^{(1)}\rho_1)Y_0 \\ &- H_n^{(2)}(k_0\rho_1)J^{(1)}(n,k_{\rm e}^{(1)}\rho_1)Y_{\rm e}^{(1)} \\ &+ \frac{J_n(k_{\rm e}^{(1)}b)}{H_n^{(2)}(k_{\rm e}^{(1)}b)}[H^{(1)}(n,k_{\rm e}^{(1)}\rho_1)H_n^{(2)}(k_0\rho_1)Y_1 \\ &- H_n'^{(2)}(k_0\rho_1)H_n^{(2)}(k_{\rm e}^{(1)}\rho_1)Y_0]\,. \end{aligned} \tag{25}$$

By defining the following function:

$$\xi_n(x,y) = \frac{Y_{\rm e}^{(1)}}{Y_0}\left[J^{(1)}(n,x) - \frac{H^{(1)}(n,x)}{H_n^{(2)}(y)}J_n(y)\right] \tag{26a}$$

$$\eta_n(x,y) = J_n(x) - \frac{H_n^{(2)}(x)}{H_n^{(2)}(y)}J_n(y) \tag{26b}$$

and noting $\rho_1 = a$, the expression (24a) is transformed into

$$A_n = -\frac{J_n(k_0a)\xi_n(k_{\rm e}^{(1)}a,k_{\rm e}^{(1)}b) - J_n'(k_0a)\eta_n(k_{\rm e}^{(1)}a,k_{\rm e}^{(1)}b)}{H_n^{(2)}(k_0a)\xi_n(k_{\rm e}^{(1)}a,k_{\rm e}^{(1)}b) - H_n'^{(2)}(k_0a)\eta_n(k_{\rm e}^{(1)}a,k_{\rm e}^{(1)}b)}\,. \tag{27}$$

For comparison with Yokota's formulae (21) and (22) given for a multi-pole field,[12] we must first derive the relationship between Tokota's and ours. Comparing the expressions (10) and (13) in Ref. [12] with the expressions (5) and (6), one has

$$\beta_m e^{j m\theta} = (-j)^n E_0 e^{-jn\varphi}, \tag{28}$$

$$C_m e^{j m\theta} = A_n (-j)^n E_0 e^{-jn\varphi}. \tag{29}$$

Dividing the expression (29) by the expression (28) leads to

$$A_n = \frac{C_m}{\beta_m}. \tag{30}$$

Substitution of expressions (21) and (22) in Ref.[12] into the expression (30) results in

$$A_n = -\frac{J_m(ka_2)\zeta - J'_m(ka_2)\eta}{H_m^{(2)}(ka_2)\zeta - H'^{(2)}_m(ka_2)\eta} \tag{31}$$

with

$$\eta = J_m(k_1 a_2) - \frac{Y_m(k_1 a_2)}{Y_m(k_1 a_1)} J_m(k_1 a_1), \tag{32a}$$

$$\zeta = D_m(k_1 a_2) - \frac{\tilde{D}_m(k_1 a_2)}{Y_m(k_1 a_1)} J_m(k_1 a_1), \tag{32b}$$

and

$$D_m(k_1 a_2) = \frac{1}{\mu_{\text{eff}}} \frac{k_1}{k} \left[ J'_m(k_1 a_2) - \frac{\kappa}{\mu} \frac{m}{k_1 a_2} J_m(k_1 a_2) \right], \tag{33a}$$

$$\tilde{D}_m(k_1 a_2) = \frac{1}{\mu_{\text{eff}}} \frac{k_1}{k} \left[ Y'_m(k_1 a_2) - \frac{\kappa}{\mu} \frac{m}{k_1 a_2} Y_m(k_1 a_2) \right]. \tag{33b}$$

Note $\frac{1}{\mu_{\text{eff}}} \frac{k_1}{k} = \frac{Y_e^{(1)}}{Y_0}$, $k_1 = k_e^{(1)}$, $k = k_0$, $\kappa = -\mu_2^{(1)}/\mu_0$, $\mu = \mu_1^{(1)}/\mu_0$, $a_2 = a$, $a_1 = b$, and replace $m$ and the Neumann function $Y_m(x)$ in Yokota's results by $n$ and the Hankel function $H_n^{(2)}(x)$, respectively, then the scattering coefficient (31) given by Yokota will turn to the expression (27).

It is interesting to consider further two particular cases, i.e. homogeneous magnetized ferrite cylinder and homogeneous dielectric-coated conducting cylinder. In the first case, we let the inner radius $b$ of the conducting cylinder approach to zero. This leads $J_n(k_e^{(1)} b)/H_n^{(2)}(k_e^{(1)} b)$ to vanish. Hence, the expression (24a) reduces to

$$A_n = \frac{J'_n(k_0 a) J_n(k_e^1 a) Y_0 - J^{(1)}(n, k_e^1 a) J_n(k_0 a) Y_e^{(1)}}{-H'^{(2)}_n(k_0 a) J_n(k_e^{(1)} a) Y_0 + H_n^{(2)}(k_0 a) J^{(1)}(n, k_e^{(1)} a) Y_e^{(1)}}, \tag{34}$$

which coincides with Eggimann's.[8]

If the ferrite is not magnetized and the magnetic bias field is zero, the ferrite acts as an isotropic dielectric with the permeability $\mu = \mu_0$. In this case, the expression (24a) reduces to

$$A_n = -\frac{J_n(k_0 a) - Z_n(k_1 a, k_1 b) J'_n(k_0 a)}{H_n^{(2)}(k_0 a) - Z_n(k_1 a, k_1 b) H'^{(2)}_n(k_0 a)} \tag{35}$$

with

$$Z_n(k_1 a, k_1 b) = \frac{Y_0}{Y_1} \frac{J_n(k_1 a) H_n^{(2)}(k_1 b) - J_n(k_1 b) H_n^{(2)}(k_1 a)}{J'_n(k_1 a) H_n^{(2)}(k_1 b) - J_n(k_1 b) H'^{(2)}_n(k_1 a)}, \tag{36}$$

where $k_1 = k_0 \sqrt{\varepsilon_r}$, and $\varepsilon_r$ is the relative dielectric constant. This result coincides with Ruch's in the case of the permeability $\mu_1 = \mu_0$.[19]

## 3. Numerical results and discussion

In the following discussion, the SMM solution is applied to simulate the electromagnetic scattering from the ferrite-coated conducting cylinder with two linear profiles

$$\frac{\mu_2}{\mu_1}(\rho) = \beta_1 + \alpha_1 \frac{\rho - b}{a - b}, \quad \varepsilon_r = \text{constant}, \tag{37}$$

and

$$\varepsilon_r(\rho) = \beta_2 + \alpha_2 \frac{\rho - b}{a - b}, \quad \frac{\mu_2}{\mu_1} = \text{constant}. \tag{38}$$

The parameters of two profiles above are chosen from Refs.[8] and [17]. When the parameter $\mu_2/\mu_1$ is equal to zero, the profile (38) presents the general inhomogeneous dielectric coating. For convenience, we refer to the profiles with $\alpha_{1,2} > 0$ as the linear increasing

profiles and the profiles with $\alpha_{1,2} < 0$ as the linear decreasing profiles.

Figure 2 shows the normalized backscattering cross section (NBSCS) as a function of the precession frequency for the linear profile (37). The parameters are the operating frequency $f = 9$GHz, the linewidths $\Delta H = 10.0 \times 10^{-3}$T, the coating thickness $d(= a - b) = 0.33$cm, $\beta_1 = 1.5$, $\varepsilon_r = 11$, and three values $\alpha_1 = 0$, –0.3, and 0.3. Also shown in this figure is the NBSCS for a dielectric-coated conducting cylinder with $\varepsilon_r = 11$ and $\mu_r = 1$ which is denoted by dotted line (similarly in the following figures). Figure 2(a) is for the inner radius $b = 2$ cm and Fig.2(b) is for the inner radius $b = 10$cm. It is clear that the minimum value of the NBSCS occurs at different applied magnetic fields for the different linear profiles. We notice that the differences in NBSCS between the ferrite coating and the dielectric coating in Fig.2(a) are bigger than those in the Fig.2(b), which results from the fact that in the first case their differences are brought about by the absorption of the ferrite and the larger power scattering in other directions, and that in the second case, we have $\lambda_0 \gg b$. So the backscattering characteristics for the ferrite coating and for the dielectric coating are similar to the characteristics of power reflection coefficients for the flat plates covered by the same material of the same thickness, respectively. Therefore, the differences in NBSCS between two coatings are mainly brought about by the absorption of the ferrite.

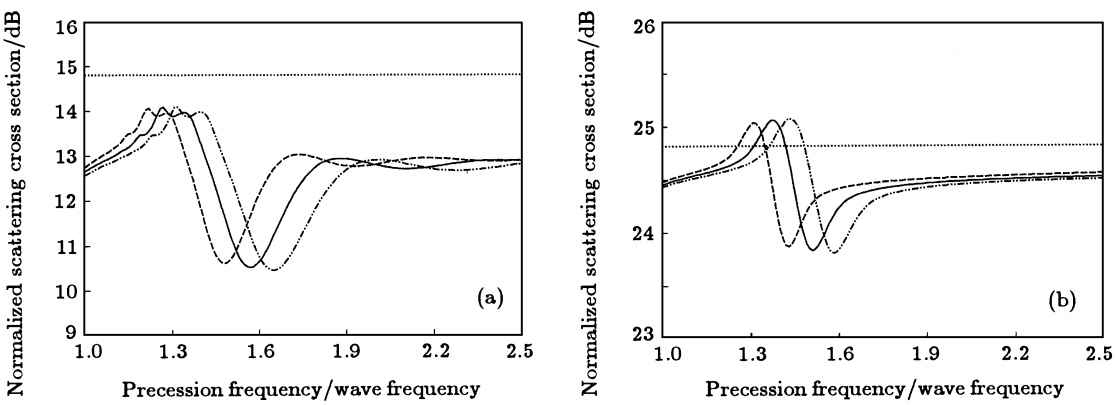



**Fig.2.** NBSCS against the precession frequency for the linear profile (37), $f$=9GHz, $\Delta H = 10.0 \times 10^{-3}$T, $d = 0.33$cm; $\varepsilon_r = 11$, $\beta_1 = 1.5$: solid line for $\alpha_1 = 0$, dashed line for $\alpha_1 = -0.3$, dotted line for $\alpha_1 = 0.3$. (a) $b = 2$cm, (b) $b = 10$cm.

Figures 3 and 4 show NBSCS as a function of the operating frequency for the coating thickness $d = 0.33$cm, the inner radius $b = 2.23$cm, the precession frequency $\omega_0 = 88.22$GHz, the linewidths $\Delta H = 10.0 \times 10^{-3}$T. Figure 3 is for the linear profile (37) with the parameters $\varepsilon_r = 11$, $\beta_1 = 1.5$, and two values $\alpha_1 = 0.3$ and –0.3. Figure 4 is for the linear profile (38) with the parameters $\beta_2 = 11$, two values $\alpha_2 = 5$, and –5, as well as $\mu_2/\mu_1 = 1.5$ for the Fig.4(a) while $\mu_2/\mu_1 = 0$ for the Fig.4(b). We see that the resonant frequency for the ferrite coating is less than that for the dielectric coating and it is a decreasing function for the ferrite parameter $\mu_2/\mu_1$. This phenomenon can be explained by the following discussion. Since the ferrite has a higher relative dielectric constant, its surface is approximately considered as a magnetic wall. The resonant condition can be obtained by letting the magnetic field be equal to zero at the ferrite surface $\rho = a$. Hence,

$$J_n(\alpha x)H_n^{(2)}(x) - J_n(x)H'^{(2)}_n - \frac{\mu_2}{\mu_1}\frac{n}{\alpha x}[J_n(\alpha x)H_n^{(2)}(x) - J_n(x)H_n^{(2)}(\alpha x)] = 0, \quad (39)$$

where $x = k_e^{(1)}b$ and $\alpha = a/b$.

If the ferrite is not magnetized and the magnetic bias field is zero, we have $\mu_2/\mu_1 = 0$. Then Eq.(39) reduces to

$$J_n(\alpha x)H_n^{(2)}(x) - J_n(x)H'^{(2)}_n = 0. \quad (40)$$

Equation (40) is the resonant condition for the dielectric coating, which has a higher dielectric constant the same as that for the ferrite coating. Comparing Eq.(39) with Eq.(40), we see that for $n = 0$ both coatings have the same roots. For $n \neq 0$ their roots are no long the same and the roots are decreasing functions for the parameter $\mu_2/\mu_1$. These results lead the resonant frequency to be a decreasing function for $\mu_2/\mu_1$.

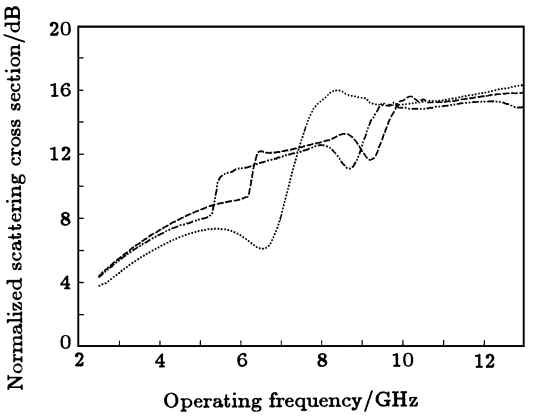



**Fig.3.** NBSCS against the operating frequency for the linear profile (37), $\omega_0 = 88.22$GHz, $\Delta H = 10.0 \times 10^{-3}$T, $d = 0.33$cm, $b = 2.23$cm; $\varepsilon_r = 11$, $\beta_1 = 1.5$: dashed line for $\alpha_1 = -0.3$, and dotted line for $\alpha_1 = 0.3$.

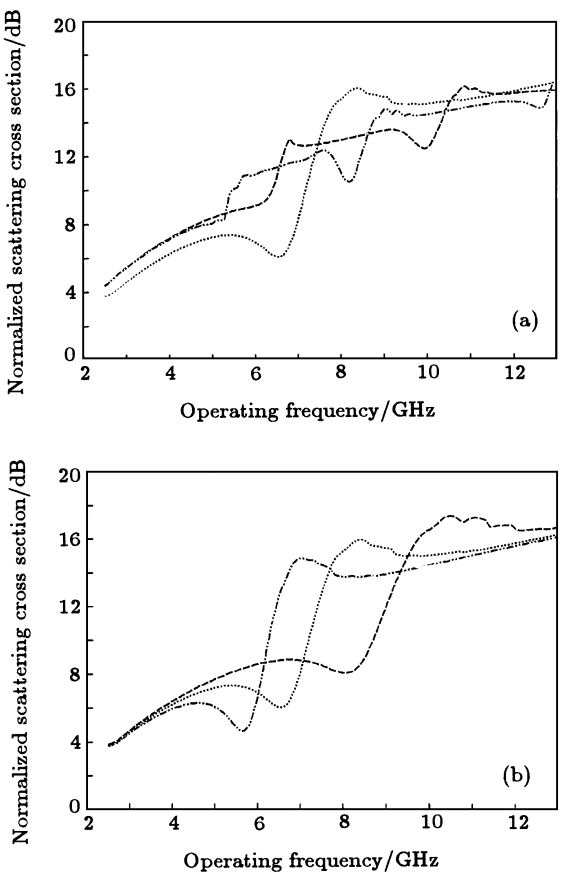



**Fig.4.** NBSCS against the operating frequency for the linear profile (38), $\omega_0 = 88.22$GHz, $\Delta H = 10.0 \times 10^{-3}$T, $d = 0.33$cm, $b = 2.23$cm; $\beta_2 = 11$: dashed line for $\alpha_2 = -5$, and dotted line for $\alpha_2 = 5$. (a) $\mu_2/\mu_1 = 1.5$, (b) $\mu_2/\mu_1 = 0$.

The other plots of the NBSCS are displayed in Fig. 5 for the nonuniform profiles (37) and (38) with the coating thickness $d = 0.33$cm, the linewidth $\Delta H = 10.0 \times 10^{-3}$T, the processing frequency $\omega_0 = 88.2$GHz, the operating frequency $f = 9$GHz, and the inner radius $b = 2$cm. Figure 5(a) is for the linear profile (37) with the parameters $\beta_1 = 1.5$, $\varepsilon_r = 11$ and two values $\alpha_1 = 0.3$ and –0.3. Figure 5(b) is for the linear profile (38) with the parameters $\beta_2 = 11$, $\alpha_2 = 5$, and two values $\mu_2/\mu_1 = 0$ and 1.5, while Fig.5(c) with $\beta_2 = 11$, $\alpha_2 = -5$, and two values $\mu_2/\mu_1 = 0$ and 1.5. These figures show that the far-field distributions for the inhomogeneous dielectric coating remain symmetrical in pattern, while the far-field distributions for the nonuniform ferrite coating remain unsymmetrical in pattern, particularly for the linear increasing profiles. These differences between the two coatings are easy to explain by the SMM formulae. To see those clearly, we rewrite expression (6) as

$$\begin{aligned} E_z^{\mathrm{s}} =& E_0 \Big\{ A_0 H_0^{(2)}(k_0\rho) \\ &+ \sum_{n=1}^{\infty} (-\mathrm{j})^n H_n^{(2)}(k_0\rho)[(A_n + A_{-n})\cos(n\varphi) \\ &+ \mathrm{j}(-A_n + A_{-n})\sin(n\varphi)] \Big\}. \end{aligned} \tag{41}$$

For the dielectric coating, we have $J^{(i)}(-n,x) = (-1)^n J_n(x)$ and $H^{(i)}(-n,x) = (-1)^n H_n^{(2)}(x)$. From the Bessel function identity and the matrix theory we know that the matrices $[S_1]$, $[S_m]$, $[S_g]$ and the vector $\{V_p\}$ are even functions of the integer $n$. These results lead the scattering coefficient $A_{-n}$ to equal $A_n$ and the sine term in the expression (41) to vanish. Then the expression (41) reduces to

$$\begin{aligned} E_z^{\mathrm{s}} =& E_0 \Big[ A_0 H_0^{(2)}(k_0\rho) \\ &+ \sum_{n=1}^{\infty} (-\mathrm{j})^n H_n^{(2)}(k_0\rho)(A_n + A_{-n})\cos(n\varphi) \Big]. \end{aligned} \tag{42}$$

This shows that the scattering field is an even function of $\varphi$. Therefore, the far-field distribution for the dielectric coating remains symmetrical in pattern. For the ferrite coating, we find that $J^{(i)}(-n,x) \neq (-1)^n J^{(i)}(n,x)$ and $H^{(i)}(-n,x) \neq (-1)^n H^{(i)}(n,x)$. These lead to the conclusion that the matrices $[S_1]$, $[S_m]$, $[S_g]$ and the vector $\{V_p\}$ are not even functions of the integer $n$. So the scattering coefficient $A_{-n}$ is unequal to $A_n$ and the sine term in (41) no long vanishes. The scattering field is the sum of the sine and cosine terms. The far-field distribution for the ferrite coating remains unsymmetrical in pattern.

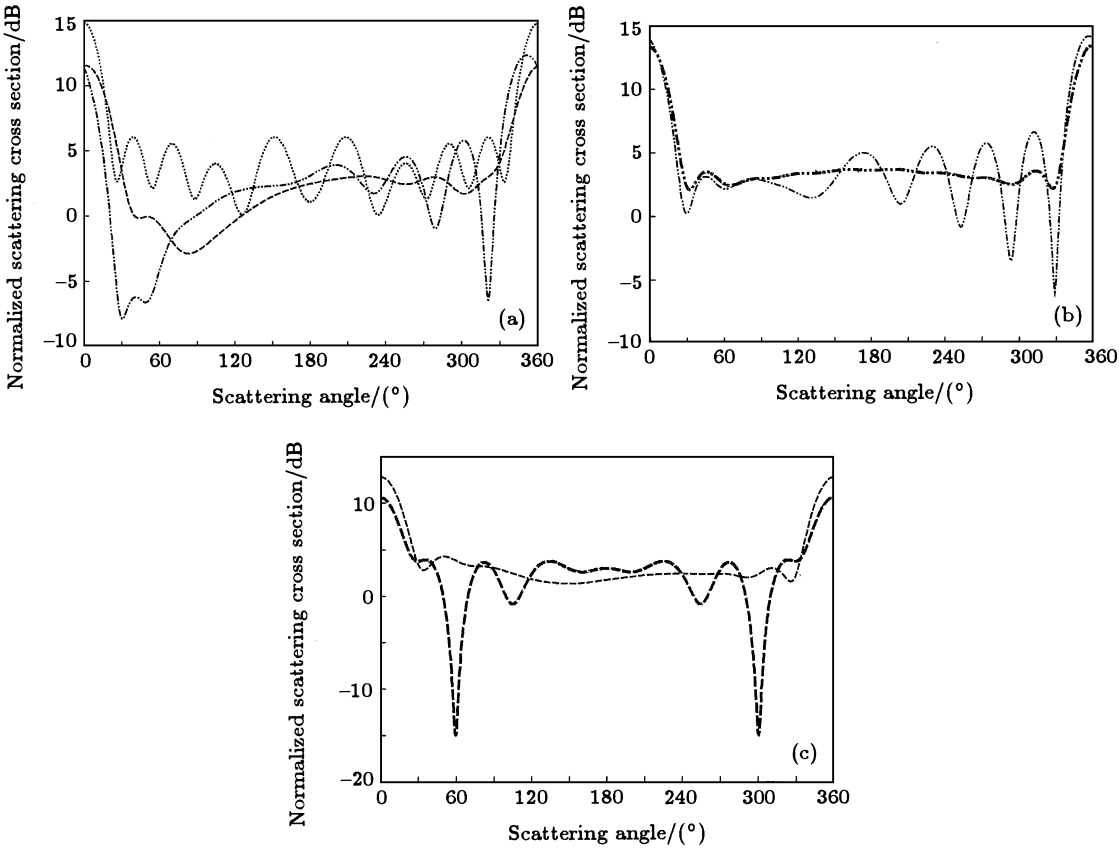



**Fig.5.** NBSCS against the scattering angle, $b = 2$cm, $d = 0.33$cm. (a) for the linear profile (37) with the same parameters as those of Fig.2(b) and Fig.2(c) for the linear profiles (38): dashed line / dotted line for the linear decreasing / increasing profiles with the same parameters as those of Fig.4(a), thick dashed line / thick dotted line for the linear decreasing / increasing profiles with the same parameters as those of Fig.4(b).

## 4. Conclusions

The so-called scattering matrix method is developed to analyse the scattering of the planar wave from the nonuniform magnetized ferrite-coated conducting cylinders. The analysis shows that the obtained SMM solution for the nonuniform ferrite coating can be reduced to the expressions for the scattering and penetrated coefficients in four particular cases: nonuniform magnetized ferrite cylinder, uniform magnetized ferrite-coated conducting cylinder, uniform ferrite cylinder as well as homogeneous dielectric-coated conducting cylinder. The resonant condition for the nonuniform ferrite coating is obtained. The characteristics of backscattering and the far-field distributions for the ferrite-coated conducting cylinder with two types of the linear profiles defined by expressions (37) and (38) are investigated versus the applied magnetic field and the wave frequency. The distinctive differences in scattering between the nonuniform ferrite coating and the nonuniform dielectric coating are demonstrated. The numerical results show that the variations of the NBSCS with the scattering angle for inhomogeneous dielectric coated conducting cylinders are slower than those for homogeneous dielectric coated conducting cylinders, while the variations of the NBSCS with the scattering angle for nonuniform magnetized ferrite coated conducting cylinders depend on the shapes of the nonuniform ferrite profiles. In view of decreasing NBSCS of the ferrite coating, an optimum nonuniform ferrite profile and an appropriate coating thickness as well as the inner radius are needed.

## References

[1] Helaly A, Soliman E A and Megahed A A 1997 *IEE Proc-H* **144** 61

[2] Laroussi M and Routh J R 1993 *IEEE Trans. Plasma Sci.* **21** 366

[3] Karbushev N I, Kolosov Y A, Polovkov A I, Selivanov I A and Shkvarunetsl A G 1992 *J. Plasma Sci.* **18** 534

[4] Hu B J, Wei G and Lai S L 1999 *IEEE Trans. Plasma Sci.* **27** 1131
[5] Morgan M A, Fisher D L and Milne E A 1987 *IEEE Trans. Antenna Propagat.* **35** 191
[6] Titchener J B and Wills J R 1991 *IEEE Trans. Antenna Propagat.* **39** 35
[7] Shen Z 1993 *Int. J. Electronics* **74** 627
[8] Eggimann W H 1960 *IRE Trans. Microwave Theory Tech.* **8** 440
[9] Okamoto N 1970 *IEEE Trans. Antenna Propagat.* **18** 642
[10] Okamoto N 1979 *IEEE Trans. Antenna Propagat.* **7** 317
[11] Eaves R E 1976 *IEEE Trans. Antenna Propagat.* **24** 190
[12] Yokota M, Takenaka T and Fukumitsu O 1987 *Radio Science* **22** 175
[13] Elshandwily M E, Kamal A A and Abdallah E A F 1973 *IEEE Trans. Microwave Theory Tech.* **21** 392
[14] Yoshida T, Umeno M and Miki S 1972 *IEEE Trans. Microwave Theory Tech.* **20** 739
[15] Okamoto N, Nishioka I and Nakanishi Y 1971 *IEEE Trans. Microwave Theory Tech.* **19** 521
[16] Bolle D M and Lewin L 1973 *IEEE Trans. Microwave Theory Tech.* **21** 118
[17] Pozar D M 1993 *Microwave Engineering* (New York: Addison-Wesley)
[18] Umashankar K and Taflove A 1993 *Computational Electromagnetics* (Boston: Artech House)
[19] Ruch G T, Barrick D E, Stuart W D and Krichbaum K 1970 *Radar Cross Section Handbook* (New York: Plenum)